cies compared with present results and it is suspected that the structural data are slightly different. However, the predicted flutter velocities are practically the same and the agreement is better than 0.5%.

Conclusions

The harmonic gradient and the source distribution methods for computing supersonic aerodynamics are compared using the F-18 as a test case. For rigid-body modes, good agreement in pressure distributions is observed except for high reduced frequencies and near the wing tip. For oscillating flaps and control surfaces, the SPIP program requires a large number of source points to give the proper pressure jump across the hinge line, while the ZONA51C code handles the sharp pressure change quite satisfactorily without requiring additional elements to be placed near the hinge line. Flutter results for the F-18 wing agree very well between these two aerodynamic methods.

Acknowledgments

The author wishes to thank the National Defence of Canada for their support and making available some F-18 data.

References

[1] Jones, W. P. and Appa, K., "Unsteady Supersonic Aerodynamic Theory for Interfering Surfaces by the Method of Potential Gradient," NASA CR-2898, 1977.

[2] Chen, P. C. and Liu, D. D., "A Harmonic Gradient Method for Unsteady Supersonic Flow Calculations," *Journal of Aircraft*, Vol. 22, May 1985, pp. 371–379.

[3] Hounjet, M. H. L., "Improved Potential Gradient Method to Calculate Airloads on Oscillating Supersonic Interfering Surfaces," *Journal of Aircraft*, Vol. 19, May 1982, pp. 390–399.

[4] Zartarian, G. and Hsu, P. T., "Theoretical Studies on the Prediction on Unsteady Airloads on Elastic Wings," WADC TR56-97, Dec. 1955.

[5] Ii, J. M., Borland, C. J., and Hogley, J. R., "Prediction of Unsteady Aerodynamic Loading of Non-Planar Wings and Wing-Tail Configurations in Supersonic Flows," Air Force Flight Dynamics Lab, TR-71-108, 1972.

[6] Garcia-Fogeda, P. and Liu, D. D., "A Harmonic Potential Panel Method for Flexible Bodies in Unsteady Supersonic Flow," AIAA Paper 86-0007, Jan. 1986.

[7] Rodden, W. P., Giesing, J. P., and Kalman, T. P., "New Developments and Applications of the Subsonic Doublet-Lattice Method for Nonplanar Configurations," *Symposium on Unsteady Aerodynamics for Aeroelastic Analyses of Interfering Surfaces*, AGARD CP 80, May 1970, Paper 4.

[8] Burkhart, T. H., "Numerical Application of Evvard's Supersonic Wing Theory to Flutter Analysis," AIAA Paper 80-0741, 1980.

[9] "Documentation of ZONA51 Code," Zona Technology, Inc., Rept. ZONA 85-1, July 1985.

[10] Potter, M., National Defence of Canada, Ottawa, Canada. Private communication, 1986.

Calculated and Experimental Stresses in Solid and Ring Slot Parachutes

William L. Garrard* and Michael L. Konicke†
University of Minnesota, Minneapolis, Minnesota

Introduction

IN the late 1960's and early 1970's Mullins and co-workers[1-3] developed a finite-element code called CANO (canopy stress analysis) to calculate the canopy shape, stresses in the horizontal ribbons, and forces in the radial members and suspension lines for ribbon parachutes. Recently, Garrard and co-workers[4-6] developed modified versions of CANO and compared the stresses and shapes calculated using these codes with experimental results for ribbon parachutes. Also, Sundberg[7] developed a new parachute stress analysis code called CALA (canopy loads analysis) that has many assumptions in common with CANO but exhibits better convergence reliability.

CANO has become the standard code for parachute stress analysis and has been used to design a variety of high-performance ribbon parchutes[8] and, more recently, solid parachutes.[9] However, one of the basic assumptions underlying both CANO and CALA is that the canopy is under uniaxial stress in the circumferential direction. This is a good assumption for ribbon parachutes but not for solid or ring-slot parachutes. Garrard and co-workers[10-12] measured stresses in both solid and simulated ring-slot parachutes, and the purpose of this Note is to compare these measured results with those obtained using various versions of CANO. To the authors' knowledge, such comparisons have not been reported. CANO and CALA have been shown to yield similar numerical results when applied to the same parachute; therefore, comparisons between CALA and the experimental results should be about the same as for CANO.

CANO requires as inputs 1) the uninflated canopy geometry, 2) the material force/deformation relationships for all canopy elements, 3) the axial load on the canopy, and 4) an estimate of the pressure distribution on the canopy. Outputs of CANO are canopy shape and forces and stresses in canopy elements. CANO begins its solution at the skirt and iteratively solves algebraic equilibrium and force/deformations relations from the skirt to the vent, trying to match two boundary conditions (one somewhat arbitrary) at the vent. CANO iteratively varies two parameters, skirt radius and magnitude of the differential pressure disibution curve, to try and converge to a solution. Since CANO starts at the skirt and tries to match a boundary condition at the vent, errors in shape at the vent can sometimes lead to errors in structural loading or convergence problems.

The solution method of CANO is as follows. The axial components of the suspension line loads balance the axial force input. Suspension line loads are determined by an iterative solution of the equilibrium and force/deformation equations for the suspension lines. Once suspension line loads have been determined, computations on the canopy proceed from the skirt to the vent. The pressure on a horizontal element is balanced by the hoop stress on the ends of this element. This hoop stress is, in turn, in equilibrium with the loads in the radial elements connected to the ends of the horizontal element. The suspension lines comprise the elements attached to the lower side of the horizontal element at the skirt. The loads in the suspension lines are known as they were calculated previously to balance the axial load. The loads and geometry of the skirt horizontal element and the radials attached to the upper side of this element are then calculated using equilibrium and compatibility between the stretched and geometrically determined length of the horizontal element. These form a coupled set of nonlinear algebraic equations that must be solved numerically. The skirt radius is iteratively adjusted until equilibrium and geometric compatibility are achieved. Then, the calculations proceed to the next horizontal element. The forces in the radials attached to the lower side of the horizontal are known from the calculations performed on the previous element, and the geometry and forces in the horizontal and the radial elements attached to its upper side are determined in the same manner as for the skirt horizontal. Calculations proceed sequentially to the vent.

Once the vent is reached, the force due to the pressure on the vent hole is calculated. If the calculated axial force component due to the radials converging at the vent is not between 25

Presented in part as Paper 86-2488 at the AIAA 9th Aerodynamic Decelerator and Balloon Technology Conference, Albuquerque, NM, Oct. 7-9, 1986; received Oct. 1, 1987; revision received April 1,1988.

*Professor, Department of Aerospace Engineering and Mechanics. Associate Fellow AIAA.

†Research Assistant, Department of Aerospace Engineering and Mechanics; currently Engineer, Boeing Commerical Airplane Co., Seattle WA. Member AIAA.

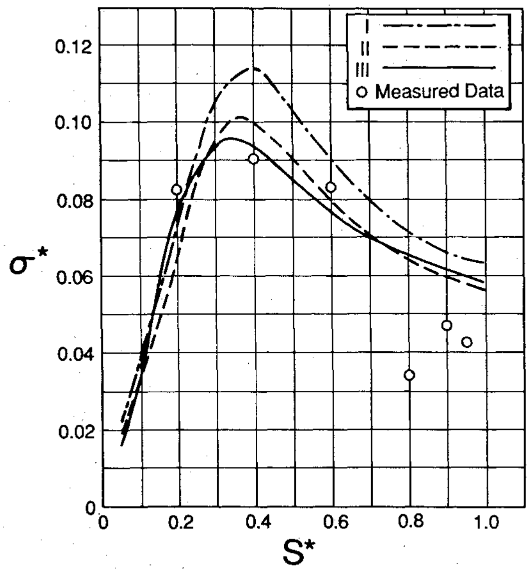

Fig. 1 Measured and calculated stress, solid parachute. Curve I: CANO3, conventional vent slope and zero skirt angle; curve II: CANO3, conventional vent slope and π/M skirt angle; curve III: CANO, conventional vent slope.

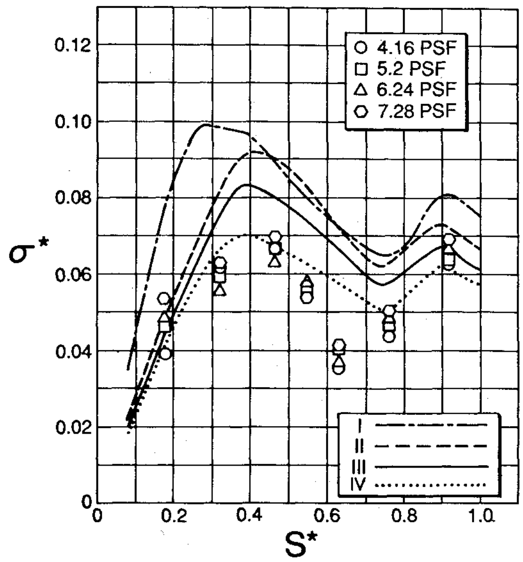

Fig. 2 Measured and calculated stress, simulated ring-slot parachute. Curve I: CANO, conventional vent slope; curve II: CANO3, conventional vent slope and zero skirt angle; curve III: CANO3, conventional vent slope and π/M skirt angle; curve IV: CANO3, modified vent slope and π/M skirt angle.

and 75% of the pressure force on the vent hole, then the magnitude of the differential pressure coefficient distribution is adjusted and the calculations for the entire canopy repeated. If the axial force lies between the specified limits, the vent length is calculated both from the canopy geometry and the force/deformation relationship for this element. If these two lengths are not sufficiently close to one another, the magnitude of the skirt radius is modified and the calculations for the entire canopy repeated. If they are acceptably close, CANO is considered to have converged. CANO is described in detail in Ref. 5.

In the study of ribbon parachutes,[4,6] canopy shapes predicted using CANO and measured shapes were found to differ substantially. This was due to differences in the slope at the vent and the angle that the horizontal ribbons made with the radials. By using the standard version of CANO, the slope at the vent can be varied by changing the allowable limits to the axial component of the force in the radials at the vent. However, in the standard version of CANO, it is impossible to change the angle the horizontals make with the radials. Since the standard version of CANO does not accurately model the angles the horizontals make with the radials, a modified version of CANO called CANO3 was developed.[4,6] This version has an option for including verticals and allows a more accurate simulation of the shape near the skirt. It has been found that a skirt angle of π/M (M is the number of gores) gives a good approximation of the canopy shape. In CANO3, the verticals are simulated as concentrated loads, not as fictitious distributed loads as in a previous modification of CANO[3]. The details of the modified versions of CANO, including the boundary conditions, are given in Ref. 6. Source code for various versions of CANO can be obtained from the senior author of this paper.

Comparison of Calculated and Experimental Results

The data from the solid parachute were taken from Ref. 10. The parachute was a 46-in.-diam, bias-constructed, solid, flat, circular parachute made up of 24 gores. The canopy was constructed of 1.1 oz/yd^2 rip-stop nylon of effective porosity of 4% (MIL-C7020-1), and the suspension lines were constructed of 100-lb nominal breaking strength nylon cord. Stress and drag were measured in the wind tunnel, but the pressure distribution was not. The stresses were measured in the warp and fill directions using Omega sensors and were then resolved into the circumferential direction. The parachute was simulated for a dynamic pressure of 7.1 psf using CANO and CANO3. Measured drag and a pressure distribution taken from Ref. 13 were used in the simulation The calculated circumferential stress was nondimensionalized by dividing by the product of the dynamic pressure and the nominal diameter. This nondimensionalized stress σ^* is plotted vs nondimensionalized distance from the apex S^* in Fig. 1. Since the shape of this parachute was not measured, only the conventional vent-slope boundary condition was used. If the shape had been known, it would have been appropriate to modify the vent-slope boundary condition. The results obtained using all versions of CANO are surprisingly good, given the assumptions.

In Ref. 11, stress measurements were performed on a 59-in.-diam slotted parachute with 24 gores constructed of the same type of material as the solid parachute just described. The parachute was block-constructed, and simulated slots were cut with a hot knife. Although the parachute was originally constructed to simulate a ribbon parachute, the construction was similar to a ring slot. Stress and drag were measured at dynamic pressures of 4.16, 5.2, 6.24, and 7.28 psf. Steady-state pressure distributions were also measured on this parachute.[12] In Fig. 2, the experimentally determined nondimensional stress is plotted vs S^* for all four dynamic pressures. The shape of the stress distribution is the same for each dynamic pressure. Stress was calculated using CANO with the conventional vent-slope boundary condition, CANO3 with zero-assumed skirt angle and conventional vent-slope boundary condition, CANO3 with skirt angle π/M and conventional vent-slope boundary condition, and CANO3 with skirt angle π/M and the vent slope adjusted to give the best approximation of the shape based on visually matching the calculated and measured shapes. All of the calculated stress distributions were the same general shape as the measured distributions, but CANO3 with an adjusted vent slope and skirt angle π/M gave the best numerical results.

Conclusion

Although CANO was not originally written for solid and ring-slot parachutes, comparison with experimental results indicates that canopy stresses are predicted accurately enough for design purposes. CANO is intended for use only with circular canopies, and there is still a need for a code predicting stresses in noncircular canopies.

Acknowledgment

This research was supported by Sandia National Laboratories under Contracts 16-9903 and 48-1974. Dr. Carl W. Peterson was contract monitor.

References

[1]Mullins, W. M., Reynolds, D. T., Lindh, K. G.,and Bottorff, M. R., "Investigation of Prediction Methods for the Loads and Stresses of Apollo Type Spacecraft Parachutes, Volume II—Stresses," NVR-6432, Northrop Corp., Newbury Park, CA, June 1970.

[2]Mullins, W. M. and Reynolds, D. T., "Stress Analysis of Parachutes Using Finite Elements," *Journal of Spacecraft and Rockets,* Vol. 8, Oct. 1971, pp. 1063–1073.

[3]Reynolds, D.T. and Mullins, W. M., "Stress Analysis of Ribbon Parachutes," AIAA Paper 75-1372, 1975.

[4]Garrard, W. L., Konicke, M. L., Wu, K. Y., and Muramoto, K. K., "Measured and Calculated Stress in a Ribbon Parachute Canopies," *Journal of Aircraft,* Vol. 24, Feb. 1987, pp. 65–72.

[5]Muramoto, K. K., and Garrard, W. L., "User's Manual CANO 2," Final Report for Sandia National Lab., Albuquerque, NM, Contract 73-0540, Jan. 1982.

[6]Garrard, W. L., Konicke, M. L., and Wu, K. Y., "A Comparison of Measured and Calculated Stress and Shape in Parachute Canopies," Final Rept. for Sandia Natational Lab., Albuquerque, NM, Contract 48-1974, Aug. 1986.

[7]Sundberg, W.D., "A New Solution Method for Steady-State Canopy Structural Loads," *Proceedings of the AIAA 9th Aerodynamic Decelerator and Balloon Technology Conference,* AIAA, New York, 1986, pp. 310–317.

[8]Meyers, S. D., Klimas, P. C., and Wolf, D. F., "Structural Analysis and Design of a High Performance Lifting Ribbon Parachute," AIAA Paper 79-0428, March 1979.

[9]Cyrus, J. D. and Nykvist, W. K., "Retrorocket-Assisted Parachute Inflight Delivery (Rapid) Systems Study," *Proceedings of the AIAA 8th Aerodynamic Decelerator and Balloon Technology Conference,* AIAA, New York, 1984, pp. 124–130.

[10]Garrard, W. L. and Konicke, T. A., "Stress Measurements in Bias Constructed Parachute Canopies During Inflation and Steady State," *Journal of Aircraft,* Vol. 18, Oct. 1981, pp. 881–887.

[11]Konicke, T. A. and Garrard, W. L., "Stress Measurements in a Ribbon Parachute Canopy," *Journal of Aircraft,* Vol. 19, July 1982, pp. 598–600.

[12]Garrard, W. L., Wu, K. Y. and Muramoto, K. K., "Steady State Stresses in Ribbon Parachutes," *Proceedings of the AIAA 8th Aerodynamic Decelerator and Balloon Technology Conference,* AIAA, New York, 1984, pp.57–67.

[13]Melzig, H. D. and Schmidt, P. K., "Pressure DistributionDuring Parachute Opening, Phase 1, Infinite Mass Case," Air Force Flight Dynamics Lab., TR-66-10, March 1966.